PHYSICAL REVIEW B **95**, 180407(R) (2017)

Bose-Einstein condensation of triplons in the $S = 1$ tetramer antiferromagnet $K_2Ni_2(MoO_4)_3$: A compound close to a quantum critical point

B. Koteswararao,[1,2,*] P. Khuntia,[3,4] R. Kumar,[5,6] A. V. Mahajan,[5] Arvind Yogi,[6] M. Baenitz,[3] Y. Skourski,[7] and F. C. Chou[2,†]

[1]*School of Physics, University of Hyderabad, Central University PO, Hyderabad 500046, India*

[2]*Center of Condensed Matter Sciences, National Taiwan University, Taipei 10617, Taiwan*

[3]*Max Planck Institute for Chemical Physics of Solids, 01187 Dresden, Germany*

[4]*Department of Physics, Indian Institute of Technology Madras, Chennai 600036, India*

[5]*Department of Physics, Indian Institute of Technology Bombay, Powai, Mumbai 400076, India*

[6]*Tata Institute of Fundamental Research, Homi Bhabha Road, Colaba, Mumbai 400005, India*

[7]*Dresden High Magnetic Field Laboratory (HLD-EMFL), Helmholtz-Zentrum Dresden-Rossendorf, 01328 Dresden, Germany*

(Received 6 March 2017; revised manuscript received 27 April 2017; published 30 May 2017)

The structure of $K_2Ni_2(MoO_4)_3$ consists of $S = 1$ tetramers formed by Ni^{2+} ions. The magnetic susceptibility $\chi(T)$ and specific heat $C_P(T)$ data on a single crystal show a broad maximum due to the low dimensionality of the system with short-range spin correlations. A sharp peak is seen in $\chi(T)$ and $C_P(T)$ at about 1.13 K, well below the broad maximum. This is an indication of magnetic long-range order, i.e., the absence of spin gap in the ground state. Interestingly, the application of a small magnetic field ($H > 0.1$ T) induces magnetic behavior akin to the Bose-Einstein condensation (BEC) of triplon excitations observed in some spin-gap materials. Our results demonstrate that the temperature-field (T-H) phase boundary follows a power law $(T - T_N) \propto H^{1/\alpha}$ with the exponent $1/\alpha$ close to $\frac{2}{3}$, as predicted for the BEC scenario. The observation of BEC of triplon excitations in small H infers that $K_2Ni_2(MoO_4)_3$ is located in the proximity of a quantum critical point, which separates the magnetically ordered and spin-gap regions of the phase diagram.

DOI: 10.1103/PhysRevB.95.180407

Spin-gap materials exhibit remarkably exotic magnetic phenomena such as the realizations of Bose-Einstein condensation (BEC) and the appearance of magnetization plateaus [1–5]. In general, spin-gap materials have a singlet ($S = 0$) ground state and the triplet excited states are separated from the ground state by an energy gap, called the spin gap. With increasing magnetic field (which leads to a Zeeman splitting of $S = 1$ states), at a critical value of the field H_c, the lowest substate of the triplet ($S_z = 1$) crosses the $S = 0$ ground state. As a result, a finite concentration of triplets (triplons) populates. This consequently leads to several field-induced magnetic long-range-ordering (LRO) phenomena such as the BEC of triplons in the vicinity of $T = 0$ K and H_c [1,2]. In this context, the applied magnetic field (H) acts as a chemical potential in separating the spin-gap region and LRO region of the quantum phase diagram at $T \to 0$ K [6]. Experimentally, field-induced BEC of triplon behavior has been intensively studied for various spin-gap materials with $S = \frac{1}{2}$ dimers $TlCuCl_3$ [7,8], $BaCuSi_2O_6$ [9,10], $Sr_3Cr_2O_8$ [11,12], and $Ba_3Cr_2O_8$ [13]. Recently, BECs of triplet and quintuplet excitations have also been observed above the critical fields 8.7 and 32.42 T, respectively, in the $S = 1$ dimer compound $Ba_3Mn_2O_8$ [14,15]. On the other hand, the BEC of magnons has been observed in other classes of materials with magnetic LRO, including yttrium-iron-garnet films at room temperature via microwave pumping [16], Cs_2CuCl_4 [17], and Gd nanocrystalline samples [18,19]. In the case of Cs_2CuCl_4, although the material undergoes a magnetic transition (T_N) at 0.595 K, the gap in the magnon spectrum closes at about 8.51 T and a three-dimensional (3D) BEC phase boundary relation $T_N \propto (H - H_c)^{1/\alpha}$ with an exponent $1/\alpha = \frac{2}{3}$ is observed, similar to other spin-gap materials [7–15]. Interestingly, when a spin-gap system is subjected to significant three-dimensional interactions, the triplet states are broadened and thus reduce the size of the spin gap. In such a case, a small H_c is enough to induce BEC of triplon excitations. This class of material offers an ideal ground to explore quantum critical phenomena in the proximity of a quantum critical point (QCP) in view of their collective spin excitations, high homogeneity in boson density, and topological order [1].

In this Rapid Communication, we study a different kind of antiferromagnetic material $K_2Ni_2(MoO_4)_3$, which exhibits magnetic LRO, through comprehensive thermodynamic studies on single crystals. Interestingly, it exhibits a field-induced BEC of triplon excitations at low magnetic fields. Being a non-spin-gap material, this quantum magnet poses to host exotic magnetic excitations and is located close to a QCP.

Polycrystalline samples of $K_2Ni_2(MoO_4)_3$ were prepared using K_2CO_3, NiO, and MoO_3. A mixture of these chemicals with a stoichiometric molar ratio of 1:2:3 was fired for 24 h with a heating rate of 60 °C per hour to reach 600 °C. The single crystals were grown using a K_2MoO_4 flux agent [see the inset of Fig. 1(a)]. The x-ray diffraction (XRD) measurements were done on both the single crystal and polycrystalline sample. The identified peaks, which correspond to $(0ll)$ planes of the $K_2Ni_2(MoO_4)_3$ phase [20], are shown in Fig. 1(a). In order to extract the unit cell lattice parameters, we have employed the Rietveld refinement analysis on the polycrystalline sample with the FULLPROF SUITE program [21] using the initial structural parameters provided by Klevtsova *et al.* in Ref. [20] [see Fig. 1(b)]. The obtained residual refinement factors R_P, R_{wp}, R_{exp}, and χ^2 are 0.177, 0.180,

*koti.iitb@gmail.com

†fcchou@ntu.edu.tw

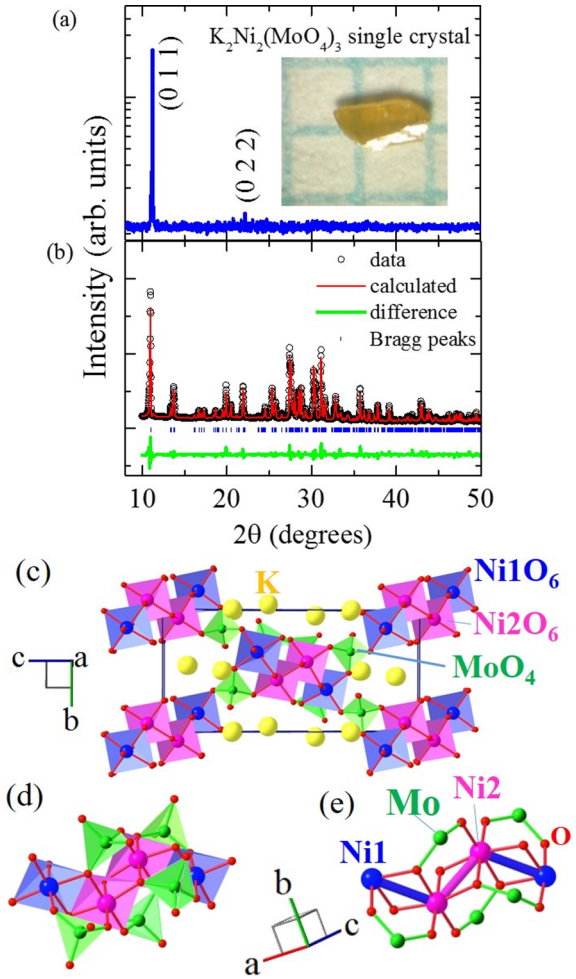

FIG. 1. (a) XRD pattern of a single crystal of $K_2Ni_2(MoO_4)_3$ with the x-ray beam perpendicular to the $(0ll)$ planes. The inset shows an image of the single crystal. The top surface is a $(0ll)$ plane. (b) Rietveld refinement of the XRD data of polycrystalline samples. (c) The crystal structure of $K_2Ni_2(MoO_4)_3$ viewed along the a direction. (d) The $S = 1$ tetramers are constructed by $Ni1O_6$ (blue) and $Ni2O_6$ (pink) octahedra. The MoO_4 tetrahedral units (green) also mediated the Ni-Ni couplings in a tetramer. (e) Representation of tetramers in the atoms and bonds.

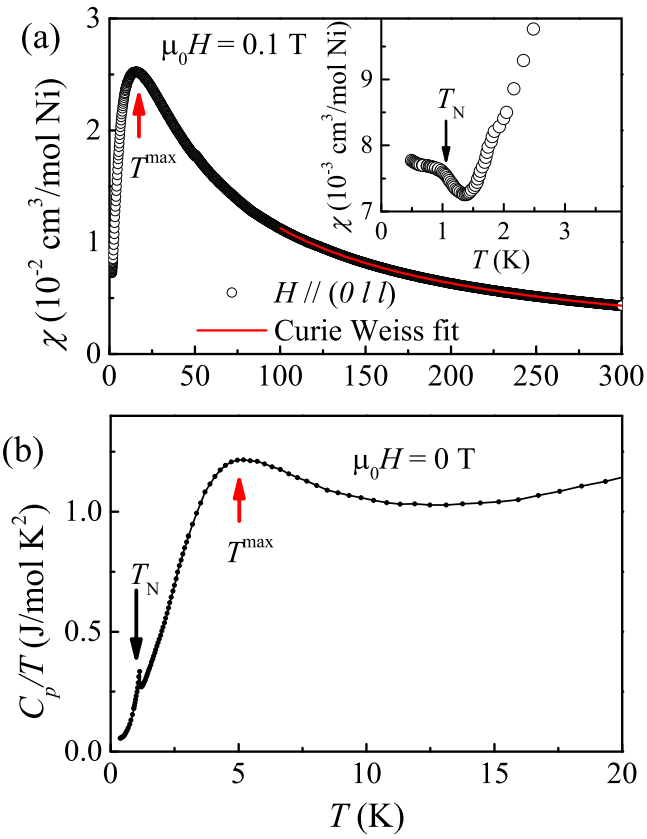

FIG. 2. (a) $\chi(T)$ of a single crystal with $H \parallel (0ll)$. The red line is a fit to the Curie-Weiss law in the T range 100–300 K. The inset shows the low-T data down to 500 mK. (b) The data of C_P/T in zero field. The down arrow indicates T_N, while the up arrow points to the broad maximum (T^{max}).

0.035, and 5.1, respectively. The lattice parameters are found to be $a = 6.952(5)$ Å, $b = 8.910(7)$ Å, $c = 19.740(10)$ Å, and $\beta = 108.065(5)^\circ$, consistent with earlier reports [20].

The compound $K_2Ni_2(MoO_4)_3$ crystallizes in the primitive monoclinic space group $P2_1/c$ (No. 14) containing $Z = 4$ formula units per unit cell [see Fig. 1(c)]. The structure has $S = 1$ (Ni^{2+}) tetramers formed by two edge-shared $Ni1O_6$ and $Ni2O_6$ octahedra [see Figs. 1(c) and 1(d)]. The bond angles of Ni-O-Ni are in between 94° and 98°, which naively suggests that the magnetic couplings might be antiferromagnetic in nature. In a tetramer unit, the Ni^{2+} ions are connected via MoO_4 tetrahedra, which might lead to magnetic frustration through next-nearest-neighbor (NNN) interactions in the tetramer. These $S = 1$ tetramers are also connected to each other through MoO_4 tetrahedral units running in all three crystallographic directions, suggesting the presence of non-negligible three-dimensional (3D) interactions.

Magnetization (M) as a function of temperature (T) is measured on the single crystal in H parallel to the $(0ll)$ plane. The magnetic susceptibility $\chi = (M/H)$ in the T range 500 mK to 300 K is shown in Fig. 2(a). At high T, the data follow the Curie-Weiss law with an effective magnetic moment (μ_{eff}) $\approx 3.34\,\mu_B$ and a Curie-Weiss temperature $\theta_{\text{CW}} \approx -25$ K. The obtained μ_{eff} value is larger than the expected value for $S = 1$ ($2.83\,\mu_B$), but is consistent with many Ni-based magnets [22,23]. The obtained θ_{CW} of -25 K indicates the presence of antiferromagnetic couplings between the Ni^{2+} ions. At low T, $\chi(T)$ shows a broad maximum around 16 K, indicative of short-range spin correlations possibly originating from the low dimensionality of the system. Below the broad maximum, the susceptibility falls steeply down to 1.4 K and then has an upturn. Unlike the spin-gap behavior expected for isolated tetramer systems [24], the data deviate from the upturn at about 1.13 K, suggesting an antiferromagnetic transition [see the inset of Fig. 2(a)]. We have also measured the magnetization in H perpendicular to the $(0ll)$ plane, but no significant anisotropy was seen. Specific heat $C_P(T)$ data measured on a single crystal in zero field are shown in Fig. 2(b). The data of C_P/T vs T show features similar to those observed in $\chi(T)$: a broad maximum at $T^{max} \approx 5$ K and a sharp transition at $T_N \approx 1.13$ K. The observed T^{max} of $C_P(T)$ is smaller than that of $\chi(T)$, as

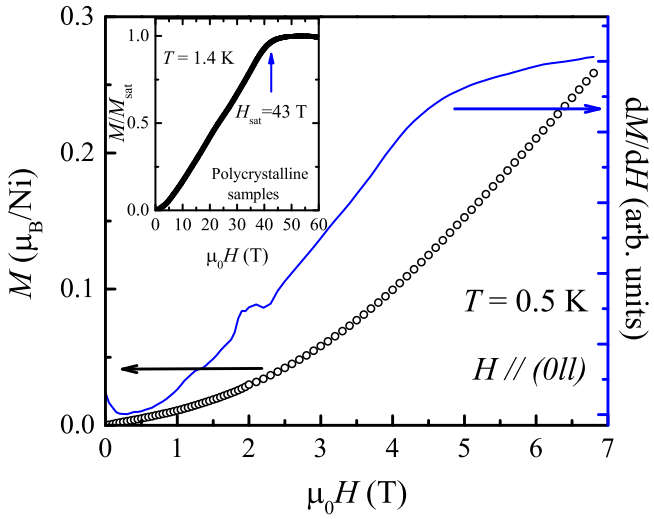

FIG. 3. (a) $M(H)$ up to 7 T at 0.5 K (left y axis). dM/dH vs H is plotted on the right y axis. The inset shows $M(H)$ data up to 60 T on a polycrystalline sample.

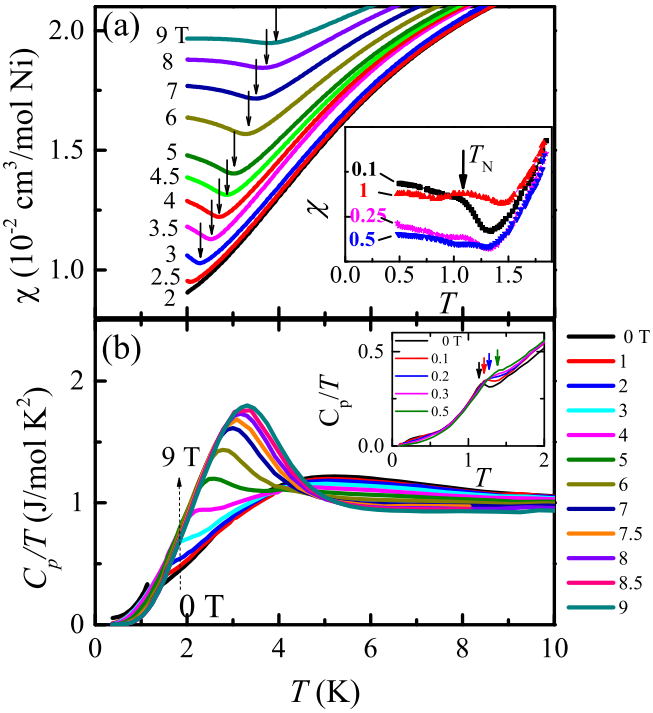

FIG. 4. (a) $\chi(T)$ data at 2–9 T. The minima in $\chi(T)$ depict a phase transition which could be reconciled as BEC of magnetic excitations. (b) C_P/T vs T for the fields from 0 to 9 T. The inset shows the data at low fields. The field-induced anomalies are represented by down arrows.

observed in other low-dimensional spin systems [25,26]. The appearance of a sharp peak at T_N infers the presence of LRO possibly due to non-negligible intertetramer interactions.

To explore further the nature of magnetic phenomena of this quantum magnet, the magnetization isotherm $M(H)$ was measured up to 7 T at $T = 0.5$ K ($<T_N$), as shown in Fig. 3. $M(H)$ data do not exhibit any hysteresis, ruling out the presence of a ferromagnetic moment. In addition, the data show a nonlinear behavior, unlike in a typical antiferromagnetic system. Similar nonlinear behavior is also seen in low fields ($H < 5$ T) in the $M(H)$ measured up to 60 T on the polycrystalline sample at 1.4 K, i.e., in the paramagnetic region ($T > T_N$), as shown in the inset of Fig. 3. The $M(H)$ data suggest the appearance of field-induced phenomenon in this quantum magnet. The magnetization increases with H and finally a fully polarized state with a saturated magnetization ($M_{\rm sat}$) about $2\,\mu_B$/Ni ($M/M_{\rm sat} = 1$) is observed beyond $H_{\rm sat} = 43$ T.

In order to understand the nature of field-induced phenomena in this material, we measured $\chi(T)$ on a single crystal in the T range 2–300 K and $C_P(T)$ down to 70 mK under fields up to 9 T. As shown in the inset of Fig. 4(a), a small H of 0.25 T suppresses the $\chi(T)$ anomaly at T_N. On further increasing H, surprisingly, the $\chi(T)$ data move to higher T and exhibit diplike anomalies, which have been observed, so far, in several spin-gap materials exhibiting the field-induced BEC of triplons (when $H > H_C$) [1,2]. The diplike anomalies or minimum in $\chi(T)$ were also evidenced by theoretical simulations to support the BEC state of triplons [7]. Similarly, a cusplike broad anomaly is observed in C_P/T data under a small H of 0.1 T [see the inset of Fig. 4(b)]. The anomaly also moves to higher temperature with increasing H. The observed transition and field-induced anomalies ($T_{\rm FI}$) from $\chi(T)$ and $C_P(T)$ data at different fields are plotted in Fig. 5(a), which separates the field-induced antiferromagnetic (FI-AFM) and paramagnetic (PM) regions. In order to evaluate the value of the critical exponent, the phase boundary is fitted with the equation $T_{\rm FI} = T_N + aH^{1/\alpha}$, where a is a proportionality factor and α is an exponent. As suggested in Ref. [27], it is to be fitted below $T < 0.4T_{\rm FI}^{\rm max}$ to get the precise exponent value. Here, $T_{\rm FI}^{\rm max}$ is the maximum temperature at which a field-induced transition can take place (the plateau in the T-H phase diagram). The obtained value of α is found to be 1.4(1), rather close to the theoretical value of the exponent $\frac{3}{2}$ predicted for 3D BEC of the universality class [27,28]. Moreover, the $T_{\rm FI}$ values almost vary linearly with $H^{2/3}$ [see the inset of Fig. 5(a)]. The observed diplike anomalies and the obtained α value suggest that the compound $K_2Ni_2(MoO_4)_3$ exhibits field-induced BEC behavior. It is interesting to notice that a very small field (0.1 T) is strong enough to induce this behavior in a system with zero-field LRO at 1.13 K.

To further understand the field-induced behavior, we have compared the data of a few spin-gap materials from the literature which exhibit a BEC of triplons (see Table I). So far, BEC behavior has been realized mostly in quantum mechanical spin-gap systems of a topological nature without any symmetry breaking. The magnetic field acts as a chemical potential and drives the density of triplons. As per the value of the spin gap and critical fields, we have positioned them in the phase diagram in Fig. 5(b). The magnetic field acts as the tuning parameter and it drives the spin-gap ground state to the AFM state via the quantum critical point (QCP) at $T \to 0$ K. It can be seen that all the existing spin-gap materials are away from the QCP as a large value of H is required to suppress the spin gap and finally to realize the field-induced phenomena. On the other hand, if any system is in the proximity of QCP, then

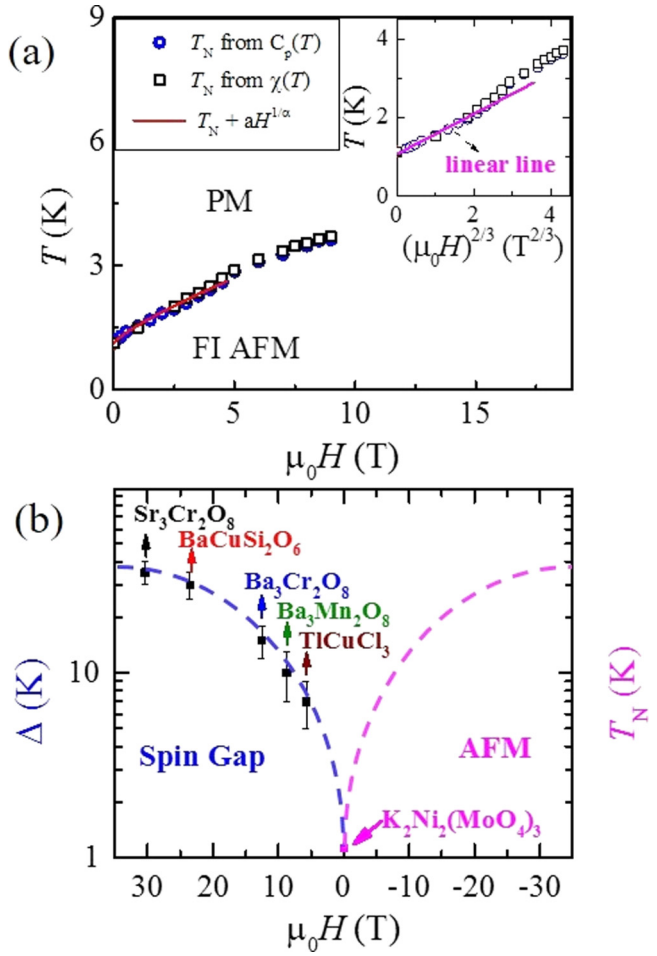

FIG. 5. (a) T-H phase diagram of $K_2Ni_2(MoO_4)_3$. The red solid line is the fit mentioned in the text. Inset: Plot of T_N vs $H^{2/3}$. The pink line is an indication of linear behavior. (b) Schematic quantum phase diagram with H as the tuning parameter. A QCP separates the spin gap and the AFM region. Some selected spin-gap compounds are on the left side of the phase diagram, while $K_2Ni_2(MoO_4)_3$ is positioned on the AFM side.

either the spin gap and/or T_N approaches zero, as shown in Fig. 5. In such a case, a small critical H would be sufficient to perturb its state. As we have already observed that a small H induces behavior akin to the BEC of triplon excitations, we conclude that $K_2Ni_2(MoO_4)_3$ is very close to the QCP on the AFM side of the quantum phase diagram. We would also like to discuss the possibility that the ground state of $K_2Ni_2(MoO_4)_3$ might have a mixture of singlets and triplets (hence causing the LRO). Due to this reason, a small amount of Zeeman energy is required for the triplon excitations. In general, BEC corresponds to the spontaneous formation of a collective state with a macroscopic number of bosons governed by a single wave function. In this antiferromagnet, the BEC of triplons state was formed probably due to the coherent precession of transverse magnetization, which breaks $U(1)$ symmetry, at zero and finite fields. Regardless of the origin of this unusual phenomenon, the system we are discussing experiences quantum mechanical fluctuations but orders at finite T. It appears to be close to the quantum critical state, i.e., an extremely small gap or transition at low T. The determination of coherence lengths via inelastic neutron scattering measurements at zero field and applied magnetic fields would be useful to further understand the BEC mechanism in this material.

TABLE I. Some details of spin-gap and antiferromagnetic materials.

Compound	Type	Δ or T_N (K)	H_c (T)	Ref.
$Sr_3Cr_2O_8$	$S = \frac{1}{2}$ dimer	35	30.4	[12]
$BaCuSi_2O_6$	$S = \frac{1}{2}$ dimer	30	23.5	[9,10]
$Ba_3Cr_2O_8$	$S = \frac{1}{2}$ dimer	15	12.5	[13]
$Ba_3Mn_2O_8$	$S = 1$ dimer	10	8.7	[15]
$TlCuCl_3$	$S = \frac{1}{2}$ dimer	7	5.7	[7]
$K_2Ni_2(MoO_4)_3$	$S = 1$ tetramer	$T_N = 1.13$	$\leqslant 0.1$	This work

We looked at several other magnetic models and the corresponding critical points. In the case of $S = \frac{1}{2}$ dimers, the magnitude of the spin gap (Δ) is the same as that of the exchange coupling (J) [29]. But, the presence of significant interdimer coupling $J'/J = 0.7$ (which is at the QCP), as in the Shastry-Sutherland model, can stabilize an AFM state [30]. In the case of the $S = \frac{1}{2}$ spin ladder, the QCP is predicted to be at a relative strength $J'/J = 0.3$ [31]. Hence, we believe that a relative intertetramer strength in $K_2Ni_2(MoO_4)_3$ might have placed it at the QCP. Moreover, the presence of NNN intratetramer couplings, which causes the magnetic frustration, does not seem to be negligible as the NiO_6 units are coupled to each other via MoO_4 units with the path Ni-O-Mo-O-Ni. The bond angles of Ni-O-Mo, O-Mo-O, and Mo-O-Ni are about 116°, 113°, and 140°, respectively, which usually favor AFM couplings [see Figs. 1(d) and 1(e)]. Magnetic frustration, which usually enhances quantum fluctuations, perhaps also plays a crucial role in placing this antiferromagnet near a QCP. Further theoretical models would help to estimate the relative strength exchange couplings to understand the origin of quantum critical behavior.

In summary, we have successfully grown single crystals of the $S = 1$ tetramer system $K_2Ni_2(MoO_4)_3$ and investigated magnetization and specific heat studies. $\chi(T)$ and zero-field $C_P(T)$ reveal that $K_2Ni_2(MoO_4)_3$ exhibits LRO at 1.13 K due to the possible involvement of non-negligible 3D couplings, in contrast to the spin-gap behavior expected for an isolated tetramer system. However, a small H of about 0.1 T induces a change in the magnetic behavior. The field-induced transition temperature increases with increasing H and follows $H^{1/\alpha}$ behavior with $\alpha = 1.4(1)$, which suggests that the observed field-induced phenomena might be related to the BEC of triplons, as observed in other spin-gap materials. Despite having LRO in zero field, the field-induced behavior even in low fields might point towards the condensation of triplon excitations with the possibility that $K_2Ni_2(MoO_4)_3$ is located in the vicinity of a quantum critical point in the phase diagram. The ground state might have a mixture of singlets and triplets, due to which a small H could induce BEC excitations in this material. We believe that our results will draw attention to explore more insights into the quantum criticality of the material discussed here.

B.K. thanks Department of Science and Technology in India for the support of INSPIRE faculty Award No. IFA14-PH-92. F.C.C. acknowledges Ministry of Science and Technology in Taiwan under Project No. MOST-104-2119-M-002-028-MY2. We thank Prof. A. Thamizhavel for providing the facilities to measure the specific heat at TIFR, Mumbai. We acknowledge the support of the HLD at HZDR, member of the European Magnetic Field Laboratory (EMFL). A.V.M. thanks Department of Science and Technology in India for financial support. We thank Prof. S. N. Kaul for helpful suggestions.

[1] T. Giamarchi, Ch. Rüegg, and O. Tchernyshyov, Nat. Phys. **4**, 198 (2008).
[2] V. Zapf, M. Jaime, and C. D. Batista, Rev. Mod. Phys. **86**, 563 (2014); **86**, 1453 (2014).
[3] H. Kageyama, K. Yoshimura, R. Stern, N. V. Mushnikov, K. Onizuka, M. Kato, K. Kosuge, C. P. Slichter, T. Goto, and Y. Ueda, Phys. Rev. Lett. **82**, 3168 (1999).
[4] K. Onizuka, H. Kageyama, Y. Narumi, K. Kindo, Y. Ueda, and T. Goto, J. Phys. Soc. Jpn. **69**, 1016 (2000).
[5] K. Kodama, M. Takigawa, M. Horvati, C. Berthier, H. Kageyama, Y. Ueda, S. Miyahara, F. Becca, and F. Mila, Science **298**, 395 (2002).
[6] S. Sachdev, *Quantum Phase Transitions* (Cambridge University Press, Cambridge, UK, 1999).
[7] T. Nikuni, M. Oshikawa, A. Oosawa, and H. Tanaka, Phys. Rev. Lett. **84**, 5868 (2000).
[8] P. Merchant, B. Normand, K. W. Krämer, M. Boehm, D. F. McMorrow, and Ch. Rüegg, Nat. Phys. **10**, 373 (2014).
[9] S. E. Sebastian, P. A. Sharma, M. Jaime, N. Harrison, V. Correa, L. Balicas, N. Kawashima, C. D. Batista, and I. R. Fisher, Phys. Rev. B **72**, 100404 (2005).
[10] M. Jaime, V. F. Correa, N. Harrison, C. D. Batista, N. Kawashima, Y. Kazuma, G. A. Jorge, R. Stein, I. Heinmaa, S. A. Zvyagin, Y. Sasago, and K. Uchinokura, Phys. Rev. Lett. **93**, 087203 (2004).
[11] Y. Singh and D. C. Johnston, Phys. Rev. B **76**, 012407 (2007).
[12] A. A. Aczel, Y. Kohama, C. Marcenat, F. Weickert, M. Jaime, O. E. Ayala-Valenzuela, R. D. McDonald, S. D. Selesnic, H. A. Dabkowska, and G. M. Luke, Phys. Rev. Lett. **103**, 207203 (2009).
[13] A. A. Aczel, Y. Kohama, M. Jaime, K. Ninios, H. B. Chan, L. Balicas, H. A. Dabkowska, and G. M. Luke, Phys. Rev. B **79**, 100409 (2009).
[14] M. Uchida, H. Tanaka, M. I. Bartashevich, and T. Goto, J. Phys. Soc. Jpn. **70**, 1790 (2001).
[15] E. C. Samulon, Y. Kohama, R. D. McDonald, M. C. Shapiro, K. A. Al-Hassanieh, C. D. Batista, M. Jaime, and I. R. Fisher, Phys. Rev. Lett. **103**, 047202 (2009).
[16] S. O. Demokritov, V. E. Demidov, O. Dzyapko, G. A. Melkov, A. A. Serga, B. Hillebrands, and A. N. Slavin, Nature (London) **443**, 430 (2006).
[17] T. Radu, H. Wilhelm, V. Yushankhai, D. Kovrizhin, R. Coldea, Z. Tylczynski, T. Luhmann, and F. Steglich, Phys. Rev. Lett. **95**, 127202 (2005).
[18] S. N. Kaul and S. P. Mathew, Phys. Rev. Lett. **106**, 247204 (2011).
[19] S. N. Kaul, Phys. Status Solidi B **248**, 2276 (2011).
[20] R. F. Klevtsova and L. A. Glinskaya, Zh. Strukt. Khim. **23**, 176 (1982).
[21] J. Rodriguez-Carvajal, Physica B **192**, 55 (1993).
[22] J. Hwang, E. S. Choi, F. Ye, C. R. Dela Cruz, Y. Xin, H. D. Zhou, and P. Schlottmann, Phys. Rev. Lett. **109**, 257205 (2012).
[23] A. Yogi, A. K. Bera, A. Maurya, R. Kulkarni, S. M. Yusuf, A. Hoser, A. A. Tsirlin, and A. Thamizhavel, Phys. Rev. B **95**, 024401 (2017).
[24] R. Becker, M. Johnsson, R. K. Kremer, H.-H. Klauss, and P. Lemmens, J. Am. Chem. Soc. **128**, 15469 (2006).
[25] B. Koteswararao, S. Salunke, A. V. Mahajan, I. Dasgupta, and J. Bobroff, Phys. Rev. B **76**, 052402 (2007).
[26] B. Koteswararao, S. K. Panda, R. Kumar, K. Yoo, A. V. Mahajan, I. Dasgupta, B. H. Chen, K. H. Kim, and F. C. Chou, J. Phys.: Condens. Matter **27**, 426001 (2015).
[27] O. Nohadani, S. Wessel, B. Normand, and S. Haas, Phys. Rev. B **69**, 220402 (2004).
[28] T. Giamarchi and A. M. Tsvelik, Phys. Rev. B **59**, 11398 (1999).
[29] D. C. Johnston, R. K. Kremer, M. Troyer, X. Wang, A. Klümper, S. L. Bud'ko, A. F. Panchula, and P. C. Canfield, Phys. Rev. B **61**, 9558 (2000).
[30] S. Miyahara and K. Ueda, Phys. Rev. Lett. **82**, 3701 (1999).
[31] S. Sachdev, Science **288**, 475 (2000).